

# High Concordance and Negative Prognostic Impact of *RAS/BRAF/PIK3CA* Mutations in Multiple Resected Colorectal Liver Metastases

Tuva Høst Brunsell,<sup>1,2,3</sup> Anita Sveen,<sup>1,2,3</sup> Bjørn Atle Bjørnbeth,<sup>2,4</sup> Bård I. Røsok,<sup>2,4</sup> Stine Aske Danielsen,<sup>1,2</sup> Kristoffer Watten Brudvik,<sup>2,4</sup> Kaja C.G. Berg,<sup>1,2,3</sup> Bjarne Johannessen,<sup>1,2,3</sup> Vanja Cengija,<sup>2,5</sup> Andreas Abildgaard,<sup>2,5</sup> Marianne Grønlie Guren,<sup>2,6</sup> Arild Nesbakken,<sup>2,3,4</sup> Ragnhild A. Lothe<sup>1,2,3</sup>

## Abstract

**We investigated the intra-patient heterogeneity of driver gene mutations among colorectal liver metastases by sequencing 479 tumor samples from 106 patients. A near-perfect intra-patient concordance was found in the mutation status of the primary tumor and multiple metastatic lesions of *KRAS/NRAS/BRAF* and *PIK3CA* when high-sensitivity methods were applied. Mutations in *KRAS* alone and *KRAS/NRAS/BRAF* combined had a negative prognostic impact after liver resection.**

**Background:** The prevalence and clinical implications of genetic heterogeneity in patients with multiple colorectal liver metastases remain largely unknown. In a prospective series of patients undergoing resection of colorectal liver metastases, the aim was to investigate the inter-metastatic and primary-to-metastatic heterogeneity of mutations in *KRAS*, *NRAS*, *BRAF*, and *PIK3CA* and their prognostic impact. **Patients and Methods:** We analyzed the mutation status among 372 liver metastases and 78 primary tumors from 106 patients by methods used in clinical routine testing, by Sanger sequencing, by next-generation sequencing (NGS), and/or by droplet digital polymerase chain reaction. The 3-year cancer-specific survival (CSS) was analyzed using the Kaplan-Meier method. **Results:** Although Sanger sequencing indicated inter-metastatic mutation heterogeneity in 14 of 97 patients (14%), almost all cases were refuted by high-sensitive NGS. Also, heterogeneity among metastatic deposits was concluded only for *PIK3CA* in 2 patients. Similarly, primary-to-metastatic heterogeneity was indicated in 8 of 78 patients (10%) using Sanger sequencing but for only 2 patients after NGS, showing the emergence of 1 *KRAS* and 1 *PIK3CA* mutation in the metastatic lesions. *KRAS* mutations were present in 53 of 106 patients (50%) and were associated with poorer 3-year CSS after liver resection (37% vs. 61% for *KRAS* wild-type;  $P = .004$ ). Poor prognostic associations were found also for the combination of *KRAS/NRAS/BRAF* mutations compared with triple wild-type ( $P = .002$ ). **Conclusion:** Intra-patient mutation heterogeneity was virtually undetected, both between the primary tumor and the liver metastases and among the metastatic deposits. *KRAS* mutations separately, and *KRAS/NRAS/BRAF* mutations combined, were associated with poor patient survival after partial liver resection.

*Clinical Colorectal Cancer*, Vol. 19, No. 1, e26-47 © 2019 The Authors. Published by Elsevier Inc. This is an open access article under the CC BY-NC-ND license (<http://creativecommons.org/licenses/by-nc-nd/4.0/>).

**Keywords:** Colorectal cancer biomarkers, Method sensitivity, Mutational status, Sequencing, Tumor heterogeneity

A.N. and R.A.L. shared last authorship.

<sup>1</sup>Department of Molecular Oncology, Institute for Cancer Research  
<sup>2</sup>K. G. Jebsen Colorectal Cancer Research Centre, Oslo University Hospital, Norwegian Radium Hospital, Oslo, Norway

<sup>3</sup>Institute for Clinical Medicine, University of Oslo, Oslo, Norway

<sup>4</sup>Department of Gastrointestinal Surgery, Oslo University Hospital, Oslo, Norway

<sup>5</sup>Department of Radiology and Nuclear Medicine, Oslo University Hospital Rikshospitalet, Oslo, Norway

<sup>6</sup>Department of Oncology, Oslo University Hospital Ullevål, Oslo, Norway

Submitted: Jan 3, 2019; Revised: Jul 11, 2019; Accepted: Sep 26, 2019; Epub: Dec 12, 2019

Address for correspondence: Ragnhild A. Lothe, PhD, Department Of Molecular Oncology, Institute for Cancer Research, Oslo University Hospital, PO Box 4950 Nydalen, Oslo N-0424, Norway  
E-mail contact: [Ragnhild.A.Lothe@rr-research.no](mailto:Ragnhild.A.Lothe@rr-research.no)

## Introduction

Resection is considered the only potentially curative treatment of colorectal liver metastases (CRLMs).<sup>1</sup> To improve survival after resection and increase the resection rates, perioperative chemotherapy has become the standard of care, often including the use of monoclonal antibodies. Resistance to antibodies targeting the epidermal growth factor receptor (EGFR) is conferred by activating mutations in the downstream regulators *KRAS* and *NRAS* (*RAS*), and possibly *BRAF* and *PIK3CA*.<sup>2,3</sup> At present, only *RAS* mutations are used as negative predictive biomarkers in clinical practice.<sup>4</sup> The clinical importance of these mutations has been reinforced by the increasing evidence of a poor prognostic impact of both *RAS* and *BRAF* mutations after resection of CRLMs.<sup>5-9</sup>

Molecular profiling is routinely performed of the primary tumor and in single metastatic lesions, without considering the subclonal evolution, resulting in potential tumor heterogeneity.<sup>10</sup> The discordance rates in *KRAS* mutations between paired primary and metastatic tumors have been reported to range from 6% to 8%.<sup>11-13</sup> However, the variation among studies has been high, and mutated subclones in the primary tumor could remain undetected owing to the low-sensitivity mutation tests currently used in the clinic. This could be an explanation for the resistance to targeted drugs in the metastatic setting, underlining the clinical importance of the identification of low-frequency mutant alleles.<sup>14-16</sup>

The genetic heterogeneity among metastases in the same patient (intra-patient inter-metastatic heterogeneity) has remained mostly unexplored in colorectal carcinoma (CRC),<sup>17</sup> although the heterogeneity of genomic aberrations and gene mutations has been suggested to have prognostic value.<sup>18,19</sup> The aim of the present study was to evaluate the prevalence and prognostic impact of intra-patient, inter-tumor heterogeneity in *KRAS*, *NRAS*, *BRAF*, and *PIK3CA* mutations using both conventional Sanger sequencing and ultrasensitive methods in patients with multiple liver metastases treated with resection.

## Patients and Methods

### Patients and Samples

All patients admitted for resection of CRLMs at Oslo University Hospital after October 2013 have been asked to participate in the ongoing SMART (screening, management, research, and translation) study, except for those patients already participating in a randomized trial of open versus laparoscopic liver resection (Oslo COMET study).<sup>20</sup> The SMART study is a prospective research project that includes tumor tissue biobanking of samples from all included patients; hence, retrospective entry is not allowed. The Oslo University Hospital is the largest hospital in Scandinavia, with responsibility for the surgical treatment of CRLMs in patients living in the South Eastern Norway Health Region, a population of 2.9 million people.

The present study of inter-tumor heterogeneity included patients participating in the SMART study from October 2013 to March 2016 and who had  $\geq 2$  resected liver metastases available for biobanking or fresh-frozen primary tumor tissue and  $\geq 1$  metastasis available. Details of patient inclusion are shown in [Figure 1](#).

Immediately after resection, tumor tissue from individual metastatic lesions  $> 5$  mm were sampled, frozen in liquid nitrogen, and stored at  $-80^{\circ}\text{C}$ . From 106 patients, a total of 394 fresh-frozen tumor samples from 372 liver metastases were available for analysis. Multiple ( $\geq 2$ ) metastatic lesions from the same resection were sampled from 97 patients, with a median of 4 lesions (range, 2-9) per patient.

A total of 17 patients had undergone surgery for the primary tumor at Oslo University Hospital and had fresh-frozen tissue samples available (1-3 per patient; total, 24 samples). Formalin-fixed paraffin-embedded (FFPE) specimens from another 61 primary tumors had been submitted for diagnostic mutation analysis of *KRAS*, *NRAS*, and *BRAF* as a part of clinical practice. Accordingly, the mutation status for the primary tumor was available for 78 of 106 patients.

The preoperative investigation included magnetic resonance imaging and/or computed tomography of the liver and the lungs, which were repeated after neoadjuvant treatment if administered. The cases of all the patients were discussed in multidisciplinary team meetings, and most patients with primarily resectable metastases received neoadjuvant and adjuvant oxaliplatin-based chemotherapy.<sup>21</sup> Patients with potentially resectable metastases at diagnosis had received conversion treatment with irinotecan- or oxaliplatin-based chemotherapy and targeted agents. Patients with extrahepatic disease were included if all metastatic tissue was considered resectable.

The follow-up protocol after surgery included computed tomography of the liver and lungs and carcinoembryonic antigen measurement every 4 months for the first year and then every 6 months for a total of 5 years.

### Ethics Approval and Consent to Participate

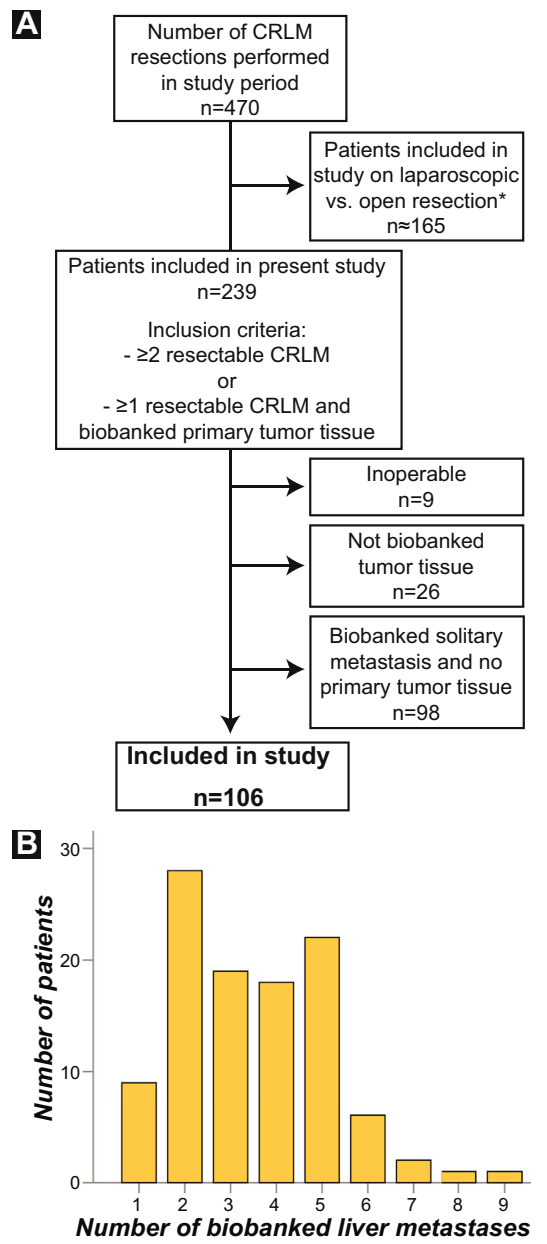
The Norwegian Data Protection Authority and the Regional Committee for Medical and Health Research Ethics, South-Eastern Norway (REC numbers: 1.2005.1629; 2010/1805) approved the present study, and all the patients provided written informed consent.

### Mutation Analyses

All mutation analyses are described in detail in the [Supplemental Appendix](#) (available in the online version) and [Supplemental Tables 1 and 2](#) (available in the online version). In brief, all 418 fresh-frozen tumor samples (394 metastatic and 24 primary) were analyzed using Sanger sequencing of *BRAF* exon 15, *KRAS* and *NRAS* exon 2-4, and *PIK3CA* exon 9 and 20. In addition, FFPE tissue from the primary tumor had been analyzed in the pathology laboratories for *KRAS* ( $n = 69$ , including 8 tumors also with fresh frozen samples), *NRAS* ( $n = 41$ ), and *BRAF* ( $n = 51$ ), with a detection limit of 1% to 10% mutant allele frequency, using different polymerase chain reaction (PCR)-based methods. Seven tumor samples were excluded because of a low tumor cell percentage.

Primary-to-metastatic mutation heterogeneity was defined as a mutation detected in  $\geq 1$  of the liver metastatic samples and not in the primary tumor samples, or vice versa. Inter-metastatic

**Figure 1** (A) Inclusion of Patients Admitted to Oslo University Hospital for Resection of Colorectal Liver Metastases. (B) Number of Biobanked Liver Metastases per Patient. \*Data from Fretland et al.<sup>20</sup>



Abbreviation: CRLM = colorectal liver metastasis.

heterogeneity was defined as a mutation detected in < 100% of all tumor samples from the liver metastases of that patient. Samples from all patients found to have either primary-to-metastatic or inter-metastatic mutation heterogeneity using Sanger sequencing (47 samples from 19 patients) were also submitted to ultra-deep targeted sequencing (Illumina TruSight Tumor 15 gene panel; Illumina, San Diego, CA) or exome sequencing. The mutation status was resolved

using these data, with a cutoff for mutations of  $\geq 0.2\%$  mutant allele frequency for targeted sequencing and 4% for exome sequencing, with at least twice the number of reads at the mutant base compared with the other bases (noise) at the same position. Additionally, predesigned droplet digital PCR (ddPCR) assays were available for 6 of the mutations that were heterogeneous according to Sanger sequencing, and mutation tests were performed using the BioRad ddPCR Assays (BioRad, Hercules, CA) in 36 samples from 9 patients.

Microsatellite instability status was determined in all tumor samples from both the primary tumors and the liver metastases using PCR analysis of the BAT25 and BAT26 markers, as previously described.<sup>22,23</sup>

**Survival Analyses**

The overall survival, 3-year cancer-specific survival (CSS), and 3-year time to recurrence (TTR) in the liver was calculated using the Kaplan-Meier method. The time to event or censoring was calculated from the start of treatment for liver metastases, which was either the date of surgical resection or the start of neoadjuvant treatment. In the CSS analyses, death from CRC was defined as an event, and patients were censored at 3 years after the start of treatment or if they had died of other causes.<sup>24</sup> In the analyses of the TTR in liver, the recurrence of liver metastasis or death from CRC were registered as events, and patients were censored after 3 years, at the last determination of their disease status, or at death from another cause.

**Statistical Analyses**

All statistical analyses were performed using IBM SPSS software, version 24.0 (IBM Corp, Armonk, NY) and included a comparison of the survival distributions using the log-rank test, multivariate Cox proportional hazards method, and Fisher exact test. Two-sided *P* values of < .05 were considered statistically significant. Owing to the low number of patients, the determination of survival according to commonly used clinical scoring systems was not performed.

**Results**

**Clinical Patient Characteristics**

A total of 106 patients, 69 men (64%) and 37 women (36%), with a median age of 67 years (range, 21-85 years) were included. Of the 106 patients, 75 (71%) had synchronous metastases discovered at or within 6 months after the diagnosis. In 18 of these patients, liver resection had been performed before resection of the primary tumor.<sup>25</sup> The median number of metastases seen on the preoperative imaging scans was 6 (range, 1-20), and the median size of the largest lesion was 3.1 cm (range, 1-16 cm).

The clinicopathologic features and treatment of the primary tumor and liver metastases are presented in Table 1. Open procedures were performed in 91 patients (86%) and laparoscopic in only 15 patients (14%), because most patients suitable for laparoscopic resection were not eligible for the present study owing to participation in another study (COMET). Two-stage procedures (ie, portal vein embolization or associating liver partition and portal vein ligation for staged hepatectomy) were performed in 29 patients (27%), and concomitant radiofrequency ablation was applied in 12 patients. Only 2 patients had been chemotherapy naive at liver resection.

**Table 1** Clinicopathologic Characteristics of Included Patients (n = 106)

Characteristic	n (%)
<b>Primary tumor location</b>	
Colon	58 (55)
Rectum	48 (45)
<b>T stage of primary tumor</b>	
pT2	7 (6.5)
pT3	74 (70)
pT4	20 (19)
Unknown	5 (4.5)
<b>N stage of primary tumor</b>	
pN0	33 (31)
pN+	69 (65)
Unknown	4 (4)
<b>Differentiation of primary tumor</b>	
Well	18 (17)
Moderate	65 (61)
Poor	8 (8)
Unknown	15 (14)
<b>Disease stage at diagnosis<sup>a</sup></b>	
I-III	15 (14)
IV	91 (86)
<b>Previous treatment</b>	
Surgery of primary tumor <sup>b</sup>	87 (82)
Neoadjuvant chemoradiotherapy	26 (25)
Chemotherapy	24 (23)
<b>Surgery of metastatic disease</b>	24 (23)
Liver	20 (19)
Lung	2 <sup>c</sup> (2)
Carcinomatosis	2 <sup>c</sup> (2)
<b>Preoperative treatment of current CRLMs</b>	
Chemotherapy	87 (82)
Oxaliplatin-based	41 (39)
Irinotecan-based	34 (32)
Both	12 (11)
Targeted treatment	36 (33)
EGFR inhibitor	12 (11)
VEGF inhibitor	21 (20)
Both	3 (3)
<b>Response (RECIST 1.1)</b>	
Partial	30 (34)
Stable disease	38 (44)
Progression	7 (8)
Unknown	12 (14)
<b>Residual disease</b>	
R0 resection of liver	
No extrahepatic disease	45 (42)
Extrahepatic disease (R2) <sup>d</sup>	11 (10)

**Table 1** Continued

Characteristic	n (%)
R1 resection of liver (< 1 mm)	
No extrahepatic disease	38 (36)
Extrahepatic disease (R2) <sup>d</sup>	8 (8)
R2 resection of liver	4 (4)

Abbreviations: CRLMs = colorectal liver metastases; EGFR = epidermal growth factor receptor; RECIST 1.1 = Response Evaluation Criteria in Solid Tumors, version 1.1; VEGF = vascular endothelial growth factor.

<sup>a</sup>Within 6 months after the diagnosis of colorectal cancer.

<sup>b</sup>All except for 2 who later underwent resection (1 with a complete response to chemoradiotherapy and 1 with progression).

<sup>c</sup>Resected simultaneously as liver metastases in 1 patient.

<sup>d</sup>R status for all locations.

### Mutation Prevalence

Mutation analysis of the liver metastasis samples from the 106 patients (with multiple metastases sampled from 97 patients) using Sanger sequencing, ultra-deep sequencing, and ddPCR analysis detected *KRAS* mutations in 53 (50%), *NRAS* mutations in 7 (6.6%), and *BRAF* mutations in 4 patients (3.8%). All these mutations were mutually exclusive, while 15 of the patients with *KRAS* exon 2-mutated tumors also had a *PIK3CA* mutation (14%). Most of the *KRAS* mutations (47 of 53; 89%) were located in exon 2. No correlation was found between these driver mutations and the number of liver lesions or the presence of extrahepatic disease. Patients with right-sided colon cancer (including the transverse colon) had more mutations in these genes than did the patients with left-sided cancer (including the rectum). Mutations were detected in 21 of 26 right-sided (81%) and 40 of 80 of left-sided (50%) cancer ( $P = .006$ ). All tumors were microsatellite stable. Details of the samples and mutations are presented in Supplemental Tables 3 and 4 (available in the online version).

Of the 4 *BRAF* mutations, 2 were located in codon 594 (D594G), a likely oncogenic mutation with possible distinct clinical associations from the more common codon 600 mutations.<sup>26-28</sup> One patient had a mutation in *KRAS* codon 33, which has been shown to display tumorigenicity in in vivo models.<sup>29</sup> However, that patient was not included as having a *KRAS* mutation in the survival analyses because of insufficient clinical data.

### Primary-to-metastatic and Inter-metastatic Mutation Heterogeneity

The analysis of 362 metastatic lesions from the 97 patients with multiple ( $\geq 2$ ) lesions sampled (Figures 2 and 3) showed that intra-patient inter-metastatic mutation heterogeneity was found in any of the 4 genes in 14 of the 97 patients (14%) using Sanger sequencing. However, ultra-deep next-generation sequencing (NGS; average coverage, 6446X for targeted and 195X for exome sequencing) and droplet digital PCR analysis identified the corresponding mutations at a low allele frequency (median, 5%; range, 0.43%-18% for NGS) in all remaining tumors from 12 of these patients (86%). Accordingly, only 2 of 97 patients had inter-metastatic mutation heterogeneity, in both cases in *PIK3CA* (additional details are provided in Supplemental Tables 3 and 4; available in the online version).

# RAS/BRAF/PIK3CA Mutations in Multiple CRLMs

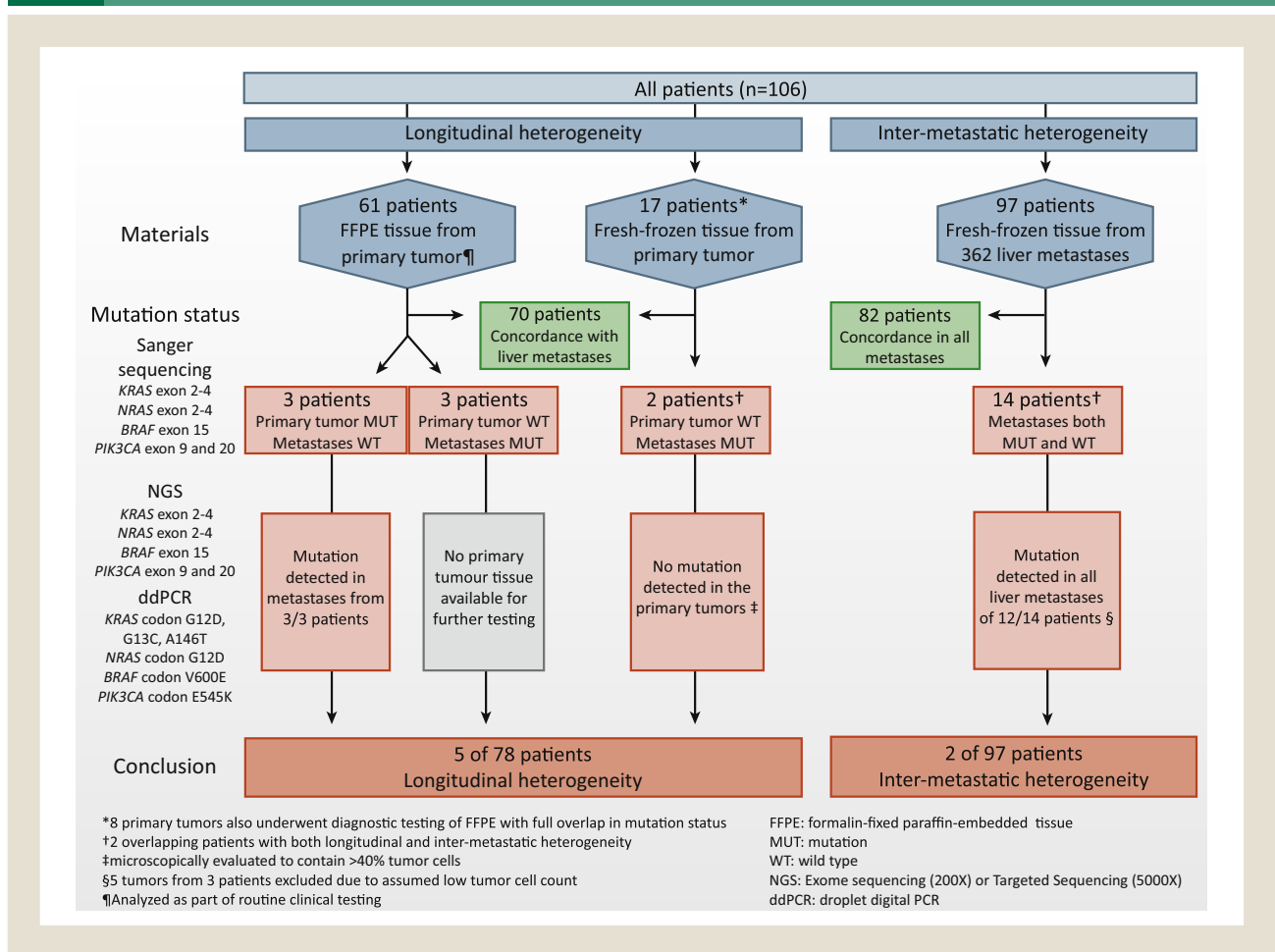
We also compared the mutation status of the primary tumor with that of the metastatic liver lesions in 78 patients (fresh-frozen primary tumor tissue available from 17 patients and the results of diagnostic testing of the primary tumor available for 61 patients). Using Sanger sequencing (Figures 2 and 3), primary-to-metastatic mutation heterogeneity in any of the 4 genes was identified in 8 of the 78 patients (10%) patients. It was found in 2 of the 17 fresh-frozen samples and 6 of the 61 FFPE samples tested in a diagnostic setting. Three of the diagnostically tested primary tumors were wild-type *KRAS* but with mutations detected in the liver metastases, resulting in a potentially false-negative predictive biomarker test result for 3 of the 61 FFPE samples (5%). The lack of available tumor tissue prevented further testing of these primary tumors. Using high-sensitivity methods on the available fresh-frozen tumor samples from the remaining patients with primary-to-metastatic mutation heterogeneity reduced the heterogeneity to 2 of 75 (3%). In both cases,

the results from the primary tumor were negative but multiple metastatic samples were positive for either a *KRAS* or *PIK3CA* mutation (Supplemental Tables 3 and 4; available in the online version). The range of mutated allele frequencies for mutations in the liver metastases not detected by Sanger sequencing was 0.20% to 1.4% (median, 0.49%) for NGS.

## Disease Recurrence and Survival

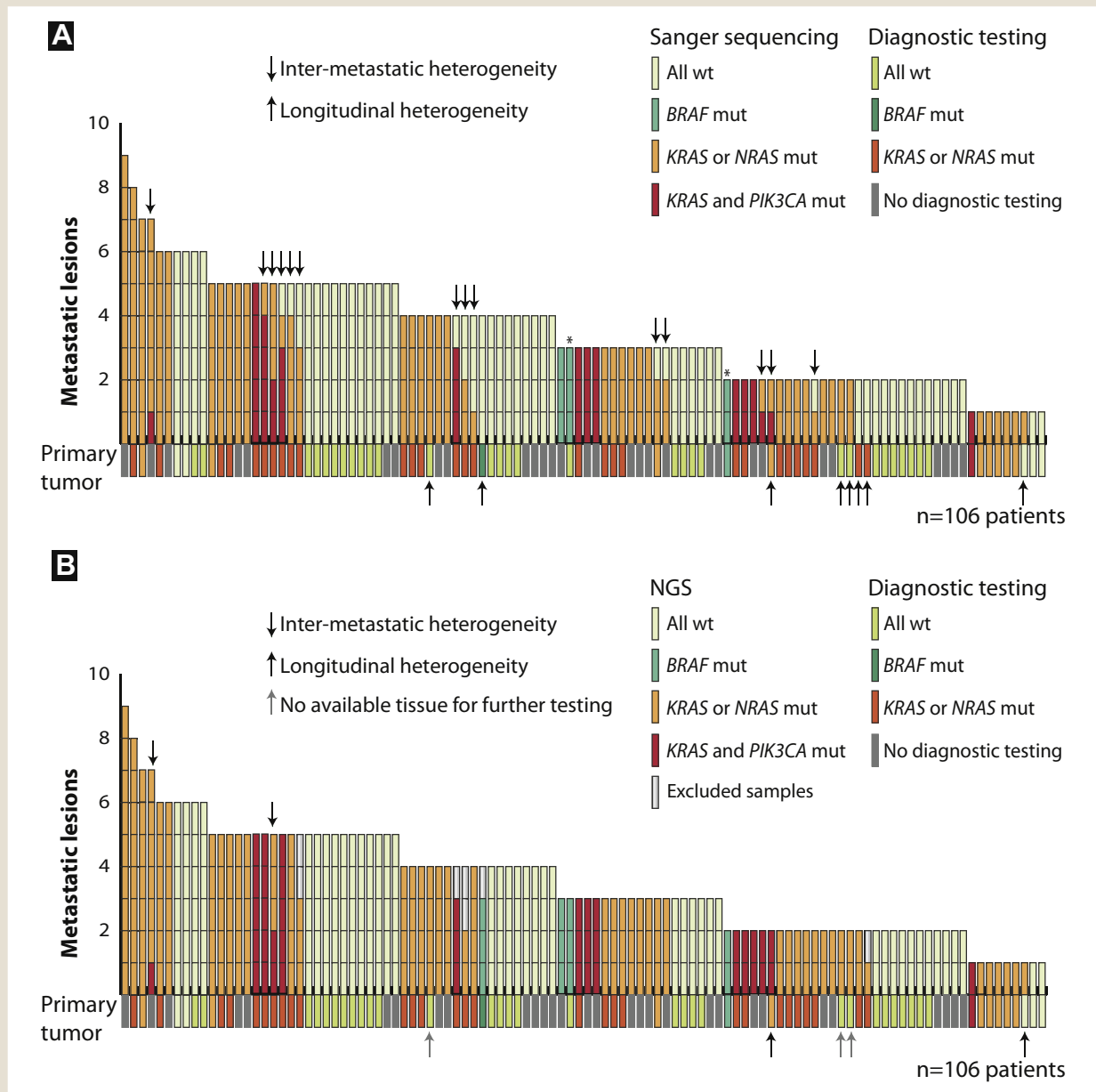
Of the 106 patients, 56 (53%) had no residual disease in the liver after resection (R0), 46 (43%) had a resection margin of < 1 mm (R1), and 4 had had residual macroscopic tumor in the liver after resection (R2). Of the patients with R0/R1 liver resection, 19 had synchronous lung or peritoneal metastases. Of these 19 patients, 4 had undergone later resection during the study period (Table 1). In the 102 patients with R0/R1 resection, recurrence in the liver was detected in 68 (67%) after a median of 11 months (range, 1-36 months). Of these 68 patients, 24 (36%) had later undergone

**Figure 2** Primary-to-metastatic and Inter-metastatic Mutation Heterogeneity of *RAS*, *BRAF*, and *PIK3CA*. \*Eight Primary Tumors Also Underwent Diagnostic Testing of FFPE With Full Overlap in Mutation Status. †Two Overlapping Patients With Both Primary-to-metastatic and Intermetastatic Heterogeneity. ‡Microscopically Evaluated to Contain > 40% Tumor Cells. §Five Tumors From 3 Patients Were Excluded Because of an Assumed Low Tumor Cell Count. ¶Analyzed as a Part of Routine Clinical Testing



Abbreviations: ddPCR = droplet digital polymerase chain reaction; FFPE = formalin-fixed paraffin-embedded; MUT = mutation; NGS = exome sequencing (200×) or targeted sequencing (5000×); WT = wild-type.

**Figure 3** Number of Metastatic Lesions per Patient With Mutations in Cancer Driver Genes. Mutations (mut) Were Detected Using (A) Sanger Sequencing and (B) Exome/Targeted Next-generation Sequencing (NGS), With Excluded Samples With an Assumed Low Tumor Cell Count Shown. The Mutation Status of the Primary Tumor According to the Diagnostic Test Results Is Shown. *BRAF* Mutations Were V600E, Except for 2 D594G Mutations, Marked With an Asterisk



Abbreviation: wt = wild-type.

resection of the recurrent liver metastases. A total of 34 patients were observed for a median of 22 months (range, 6-36 months) without evidence of metastatic liver recurrence. A total of 46 patients (43%) had developed extrahepatic recurrence, most (34 of 46; 74%) to the lungs. Only 14 patients (13% of all 106 patients) were disease-free (without hepatic or extrahepatic recurrence) throughout the study period. Four of these patients had died of other causes (ie, liver failure, sepsis, comorbidity).

The median overall survival was 36 months, with a median follow-up time of 35 months. The estimated 3-year CSS was 49% overall and was 71% after R0 resection in liver and no evidence of extrahepatic disease, 35% after R1 resection ( $P = .007$ ), and 31% after R2 resection (ie, macroscopic intra- and/or extrahepatic residual disease). The median interval to recurrence in the liver was 15 months (95% confidence interval, 12-18), with an estimated 3-year TTR in the liver of 16%.

# RAS/BRAF/PIK3CA Mutations in Multiple CRLMs

## Mutation Status and Survival

Patients with metastases harboring a *KRAS* mutation (n = 53; 50%) had significantly poorer survival compared with that of patients with *KRAS* wild-type tumors, with a 3-year CSS of 37% and 61%, respectively ( $P = .004$ ; Figure 4A). The 6 patients with *KRAS* codon 13 mutations had a 3-year CSS of 22%. For the multivariable analyses, age and potentially prognostic factors with  $P < .10$  on univariate analyses were included. The final model include age, R status, and number of liver metastases and showed that the presence of a *KRAS* mutation was a significant, independent, and negative prognostic factor for 3-year CSS (hazard ratio, 3.3; 95% confidence interval, 1.6-6.5;  $P = .001$ ).

The low prevalence of *BRAF* and *NRAS* mutations precluded meaningful analyses of the prognostic impact of these factors alone. Nevertheless, mutated *KRAS*, *NRAS*, and *BRAF* were mutually exclusive and regulate the same signaling pathway. Therefore, we tested the prognostic impact of a *KRAS*, *NRAS*, or *BRAF* mutation versus all wild-type samples. We again found a strong prognostic impact of mutation for each gene, with a 3-year CSS of 38% versus 66% ( $P = .002$ ; Figure 4B).

*PIK3CA* mutations, which had affected fewer than one third of the patients with *KRAS* mutations, were associated with reduced survival (3-year CSS, 28% vs. 52% for wild-type *PIK3CA*;  $P = .037$ ). However, the survival difference was not significant when comparing those with *KRAS* and *PIK3CA* mutations to patients with mutations in *KRAS/NRAS/BRAF* and wild-type *PIK3CA* (3-year CSS, 28% vs. 40%;  $P = .37$ ; Figure 4C).

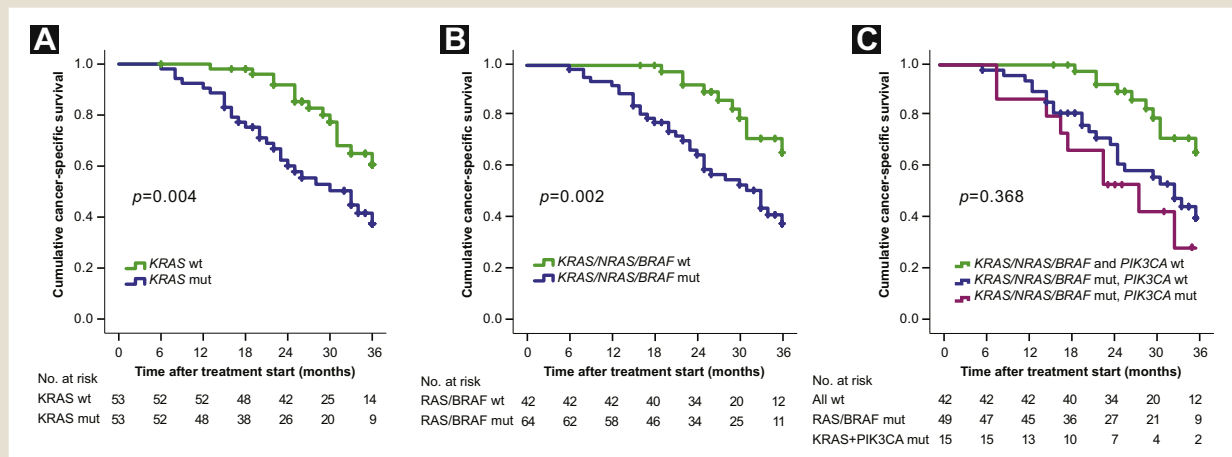
## Discussion

In a series of patients who had undergone surgical resection for liver metastases from CRC, we conducted a detailed examination of the intra-patient and inter-metastatic heterogeneity of the driver gene mutations. We found no inter-metastatic

heterogeneity for *KRAS*, *NRAS*, or *BRAF* mutations. However, we have also confirmed that heterogeneity scoring is highly dependent on the depth of the mutation analyses. The 14% heterogeneity level detected using Sanger sequencing is in concordance with the findings from the only comparable study of inter-metastatic heterogeneity of these mutations.<sup>19</sup> However, highly sensitive mutation analyses reduced the heterogeneity rate to only 2% of our patients.

Thus, the *RAS* and *BRAF* mutations were homogeneous with respect to the presence or absence of mutations in all liver metastases but heterogeneous with respect to their allelic fractions among the metastatic deposits from the individual patients. This might explain the previously reported greater prevalence of heterogeneity among metastatic tumor samples,<sup>19</sup> owing to the use of low-sensitivity methods. Low-sensitivity methods have been demonstrated to detect < 50% of the mutations that can be detected with high-sensitivity methods.<sup>30</sup> In the present study, the median of the mutated allele frequencies found was < 5% for the mutations detected using ultra-deep NGS but not using Sanger sequencing. The heterogeneity of the mutated allele fractions could also explain why 5% of the patients considered to have wild-type *KRAS* for the primary tumor in a clinical routine setting were found to have *KRAS*-mutated metastases. In the clinical setting, 1 sample from the primary tumor will usually be tested to predict the effect of anti-EGFR therapy on metastases. Pooled analyses from several studies comparing *KRAS* mutation status in the primary tumor and distant metastases have demonstrated false-positive and false-negative results, with a concordance rate from 81% to 97%, depending on the mutation test method used.<sup>11</sup> Routine diagnostic testing can fail to detect clinically relevant subclones in patients in whom resistance is developing.<sup>31-33</sup> A subclone fraction as low as 1% for *RAS* pathway genes has been suggested to result in resistance to anti-EGFR therapy in CRC, with an inverse correlation between the

**Figure 4** Three-year Cancer-specific Survival Stratified by (A) *KRAS*, (B) *KRAS*, *NRAS*, and *BRAF*, and (C) *KRAS*, *NRAS*, *BRAF*, and *PIK3CA* Mutation (mut) Status. *P* Values of *KRAS/NRAS/BRAF* Mutation With Wild-type (wt) *PIK3CA* Versus *KRAS* and *PIK3CA* Mutation Indicated



mutated subclone fraction and the response.<sup>34-36</sup> Accordingly, the mutation detection threshold for the prediction of efficacy of anti-EGFR therapy should be prospectively investigated.

The heterogeneity of mutated allele fractions among tumor lesions might result from subclonal expansion during metastatic progression, possibly affected by systemic treatment. Resistance to targeted treatment has been shown to emerge when the mutant subclone has expanded, which commonly occurs within the first months and is almost inevitable.<sup>32,37</sup> In the present study, anti-EGFR therapy had been administered to only 1 of the patients with wild-type primary tumor and *RAS*-mutated liver metastases. Thus, the treatment might explain the mutation detected in the liver metastases, which had resulted from clonal expansion and acquired resistance. Heterogeneous allele fractions might also reflect sampling bias and variation in the tumor cell percentage in the samples. Anyway, these findings suggest that the use of sensitive mutation detection methods might improve the accuracy and interpretation of clinical biomarkers. The results from several studies support our findings that *RAS* and *BRAF* mutations are homogeneous among metastases, provided that high-sensitivity methods have been used,<sup>38,39</sup> which has also been the case for other cancer types.<sup>40</sup> Studies with conflicting results have used low-sensitivity analyses<sup>19</sup> or have included very few tumor samples.<sup>41</sup>

However, the “true” inter-metastatic heterogeneity of *PIK3CA* mutations in 2 of our patients (2%) highlight the potential for mutation heterogeneity of other driver genes, which was also shown in a recent study.<sup>42</sup> Patients with inter-metastatic mutation heterogeneity using Sanger sequencing did not have poorer survival compared with those patients with homogeneous mutations (data not shown). Although in contrast to a previous study,<sup>19</sup> this supports our conclusion that the results from Sanger sequencing will not reflect the “true” mutation heterogeneity. The cases with mutation heterogeneity detected using high-sensitivity methods seemed to identify a poor prognostic subgroup. However, no conclusions could be drawn owing to the low number of patients. No significant differences in survival were found between patients with synchronous and metachronous disease (data not shown). Also, among the few patients with mutation heterogeneity, the temporal nature of the disease had no effect, in line with the findings from previous studies.<sup>43-45</sup>

Nevertheless, heterogeneity in CRC beyond driver gene mutations has been demonstrated and is likely to affect tumor progression and the response to treatment. A large number of subclones in the primary tumor, which correlated with a high degree of heterogeneity,<sup>46</sup> and the heterogeneity of genome-wide copy number aberrations<sup>18</sup> have both been associated with a poor prognosis. We have also demonstrated that intermetastatic heterogeneity in response to neoadjuvant treatment will be associated with poor survival after resection of CRLMs.<sup>47</sup> This response heterogeneity was not explained by the heterogeneity in these driver genes, indicating that several aspects of heterogeneity can be associated with disease behavior and prognosis.

The presence of a *KRAS* mutation in liver metastases had a negative prognostic impact in patients who had undergone resection for CRLMs, in accordance with the findings from several other studies.<sup>5-9</sup> Most previous studies of *KRAS* mutations and

prognosis after resection have reported on retrospective cohorts, often selecting patients who had undergone mutation testing in the clinical setting. Additionally, mutation status has usually been analyzed in the primary tumor only and/or using low-sensitivity methods, resulting in a lower *KRAS* mutation prevalence than detected in the present cohort. To the best of our knowledge, the present study is the first to show the prognostic significance of *KRAS* mutations in multiple resected CRLMs analyzed using high-sensitivity methods. In patients with primarily resectable liver metastases, EGFR blockade has no known clinical benefit and is administered only to patients with potentially resectable or unresectable metastases.<sup>48</sup> Thus, *KRAS*, in addition to being a predictive marker, is a prognostic biomarker for patients undergoing resection of CRLMs, irrespective of the use of systemic treatment.

The present study included patients with multiple liver metastases that were large enough for biobanking and molecular analyses and excluded most patients who had undergone laparoscopic resection of metastases. Accordingly, our patients had a tumor load that was greater than the average, which might explain the greater rate of positive resection margins and inferior survival compared with other unselected patient series.

## Conclusion

The intra-patient concordance in mutation status of the cancer genes *KRAS*, *NRAS*, *BRAF*, and *PIK3CA* was proved to be very high in CRLMs when using high-sensitivity methods, both between the primary tumor and the liver metastases and among multiple liver metastases. Homogeneous *KRAS* mutation of liver metastases has been shown to have a negative prognostic impact after resection of CRLMs.

## Clinical Practice Points

- Mutations in *KRAS*, *NRAS*, and, possibly, *BRAF* have been shown to confer resistance to EGFR inhibitors in CRC liver metastases.
- Previous studies, using methods with varying sensitivity, have reported discordance in mutation status among multiple liver metastases in 14% and between the primary tumor and liver metastases in 6% to 8% of patients.
- We found that the mutation status of the mutually exclusive *KRAS*, *NRAS*, and *BRAF* genes is not dependent on the lesion profiled in resectable CRLMs, owing to the near-perfect intra-patient concordance in mutation status of the primary tumor and multiple metastatic lesions, provided that highly sensitive methods are used (NGS and digital droplet PCR).
- Comparing the corresponding diagnostic data using less-sensitive methods with those using high-sensitivity methods has revealed false results, with obvious clinical relevance for prediction and prognosis; hence, only high-sensitivity methods should be applied in the clinical setting.
- We have also confirmed the negative prognostic value of *KRAS* after resection of CRLMs, alone or combined with *NRAS* and *BRAF*, in line with previous findings.



## Acknowledgments

The present study was supported by Stiftelsen Kristian Gerhard Jebsen, the Southern and Eastern Norway Regional Health Authority, the Norwegian Cancer Society (project no. 6824048-2016 to A.S. and project no. 182759-2016 to R.A.L.), and the University of Oslo/Research Council of Norway (FRIPRO Toppforsk; project no. 250993 to R.A.L.). The funding sources had no role in the study design; collection, analysis, or interpretation of the data; writing of the report; or the decision to submit the report for publication. The authors thank Magdalena Kowalewska-Harbiyeli and Gyda G. Christiansen for their assistance in patient inclusion, biobanking, and clinical data registration. They also thank Merete Hektoen, Mette Eknæs, and Merete Bjørnslett for technical assistance.

## Supplemental Data

Supplemental appendix and tables accompanying this article can be found in the online version at <https://doi.org/10.1016/j.clcc.2019.09.003>.

## Disclosure

The authors declare that they have no competing interests.

## References

- de Ridder JAM, van der Stok EP, Mekenkamp LJ, et al. Management of liver metastases in colorectal cancer patients: a retrospective case-control study of systemic therapy versus liver resection. *Eur J Cancer* 2016; 59:13-21.
- Thekildsen C, Bergmann TK, Henriksen-Schnack T, Ladelund S, Nilbert M. The predictive value of KRAS, NRAS, BRAF, PIK3CA and PTEN for anti-EGFR treatment in metastatic colorectal cancer: a systematic review and meta-analysis. *Acta Oncol* 2014; 53:852-64.
- Yang Z-Y, Wu X-Y, Huang Y-F, et al. Promising biomarkers for predicting the outcomes of patients with KRAS wild-type metastatic colorectal cancer treated with anti-epidermal growth factor receptor monoclonal antibodies: a systematic review with meta-analysis. *Int J Cancer* 2013; 133:1914-25.
- Van Cutsem E, Cervantes A, Adam R, et al. ESMO consensus guidelines for the management of patients with metastatic colorectal cancer. *Ann Oncol* 2016; 27:1386-422.
- Passiglia F, Bronte G, Bazan V, Galvano A, Vincenzi B, Russo A. Can KRAS and BRAF mutations limit the benefit of liver resection in metastatic colorectal cancer patients? A systematic review and meta-analysis. *Crit Rev Oncol Hematol* 2016; 99:150-7.
- Andreatos N, Ronnekleiv-Kelly S, Margonis GA, et al. From bench to bedside: clinical implications of KRAS status in patients with colorectal liver metastasis. *Surg Oncol* 2016; 25:332-8.
- Passot G, Denbo JW, Yamashita S, et al. Is hepatectomy justified for patients with RAS mutant colorectal liver metastases? An analysis of 524 patients undergoing curative liver resection. *Surgery* 2017; 161:332-40.
- Tosi F, Magni E, Amatu A, et al. Effect of KRAS and BRAF mutations on survival of metastatic colorectal cancer after liver resection: a systematic review and meta-analysis. *Clin Colorectal Cancer* 2017; 16:e153-63.
- Brudvik KW, Kopetz SE, Li L, Conrad C, Aloia TA, Vauthey JN. Meta-analysis of KRAS mutations and survival after resection of colorectal liver metastases. *Br J Surg* 2015; 102:1175-83.
- Jeanter M, Tougeron D, Tachon G, et al. High intra- and inter-tumoral heterogeneity of RAS mutations in colorectal cancer. *Int J Mol Sci* 2016; 17:E2015.
- Mao C, Wu X-Y, Yang Z-Y, et al. Concordant analysis of KRAS, BRAF, PIK3CA mutations, and PTEN expression between primary colorectal cancer and matched metastases. *Sci Rep* 2015; 5:8065.
- Baas JM, Krens LL, Guchelaar H-J, Morreau H, Gelderblom H. Concordance of predictive markers for EGFR inhibitors in primary tumors and metastases in colorectal cancer: a review. *Oncologist* 2011; 16:1239-49.
- Han C-B, Li F, Ma J-T, Zou H-W. Concordant KRAS mutations in primary and metastatic colorectal cancer tissue specimens: a meta-analysis and systematic review. *Cancer Invest* 2012; 30:741-7.
- Misale S, Di Nicolantonio F, Sartore-Bianchi A, Siena S, Bardelli A. Resistance to anti-EGFR therapy in colorectal cancer: from heterogeneity to convergent evolution. *Cancer Discov* 2014; 4:1269-80.
- Molinari F, Felicioni L, Buscarino M, et al. Increased detection sensitivity for KRAS mutations enhances the prediction of anti-EGFR monoclonal antibody resistance in metastatic colorectal cancer. *Clin Cancer Res* 2011; 17:4901-14.
- Tougeron D, Lecomte T, Pages JC, et al. Effect of low-frequency KRAS mutations on the response to anti-EGFR therapy in metastatic colorectal cancer. *Ann Oncol* 2013; 24:1267-73.
- Goasguen N, de Chaisemartin C, Brouquet A, et al. Evidence of heterogeneity within colorectal liver metastases for allelic losses, mRNA level expression and in vitro response to chemotherapeutic agents. *Int J Cancer* 2010; 127:1028-37.
- Sveen A, Løes IM, Alagaratnam S, et al. Intra-patient inter-metastatic genetic heterogeneity in colorectal cancer as a key determinant of survival after curative liver resection. *PLoS Genet* 2016; 12:e1006225.
- Løes IM, Immervoll H, Sorbye H, et al. Impact of KRAS, BRAF, PIK3CA, TP53 status and intraindividual mutation heterogeneity on outcome after liver resection for colorectal cancer metastases. *Int J Cancer* 2016; 139:647-56.
- Fretland AA, Dagenborg VJ, Bjørnelv GMW, et al. Laparoscopic versus open resection for colorectal liver metastases: the Oslo-COMET randomized controlled trial. *Ann Surg* 2018; 267:199-207.
- Nordlinger B, Sorbye H, Glimelius B, et al. Perioperative FOLFOX4 chemotherapy and surgery versus surgery alone for resectable liver metastases from colorectal cancer (EORTC 40983): long-term results of a randomised, controlled, phase 3 trial. *Lancet Oncol* 2013; 14:1208-15.
- De Sousa E Melo F, Wang X, Jansen M, et al. Poor-prognosis colon cancer is defined by a molecularly distinct subtype and develops from serrated precursor lesions. *Nat Med* 2013; 19:614-8.
- Merok MA, Ahlquist T, Røyrvik EC, et al. Microsatellite instability has a positive prognostic impact on stage II colorectal cancer after complete resection: results from a large, consecutive Norwegian series. *Ann Oncol* 2013; 24:1274-82.
- Punt CJA, Buyse M, Köhne C-H, et al. Endpoints in adjuvant treatment trials: a systematic review of the literature in colon cancer and proposed definitions for future trials. *J Natl Cancer Inst* 2007; 99:998-1003.
- Labori KJ, Guren MG, Brudvik KW, et al. Resection of synchronous liver metastases between radiotherapy and definitive surgery for locally advanced rectal cancer: short-term surgical outcomes, overall survival and recurrence-free survival. *Colorectal Dis* 2017; 19:731-8.
- Ng PK, Li J, Jeong KJ, et al. Systematic functional annotation of somatic mutations in cancer. *Cancer Cell* 2018; 33:450-62.e10.
- Cremolini C, Di Bartolomeo M, Amatu A, et al. BRAF codons 594 and 596 mutations identify a new molecular subtype of metastatic colorectal cancer at favorable prognosis. *Ann Oncol* 2015; 26:2092-7.
- Haley L, Tseng LH, Zheng G, et al. Performance characteristics of next-generation sequencing in clinical mutation detection of colorectal cancers. *Mod Pathol* 2015; 28:1390-9.
- Kim E, Ilic N, Shrestha Y, et al. Systematic functional interrogation of rare cancer variants identifies oncogenic alleles. *Cancer Discov* 2016; 6:714-26.
- Vanova B, Kalman M, Jasek K, et al. Droplet digital PCR revealed high concordance between primary tumors and lymph node metastases in multiplex screening of KRAS mutations in colorectal cancer. *Clin Exp Med* 2019; 19:219-24.
- Dijkstra JR, Heideman DA, Meijer GA, et al. KRAS mutation analysis on low percentage of colon cancer cells: the importance of quality assurance. *Virchows Arch* 2013; 462:39-46.
- Diaz LA Jr, Williams RT, Wu J, et al. The molecular evolution of acquired resistance to targeted EGFR blockade in colorectal cancers. *Nature* 2012; 486:537-40.
- Van Emburgh BO, Arena S, Siravegna G, et al. Acquired RAS or EGFR mutations and duration of response to EGFR blockade in colorectal cancer. *Nat Commun* 2016; 7:13665.
- Laurent-Puig P, Pekin D, Normand C, et al. Clinical relevance of KRAS-mutated subclones detected with picodroplet digital PCR in advanced colorectal cancer treated with anti-EGFR therapy. *Clin Cancer Res* 2015; 21:1087-97.
- Azuara D, Santos C, Lopez-Doriga A, et al. Nanofluidic digital PCR and extended genotyping of RAS and BRAF for improved selection of metastatic colorectal cancer patients for anti-EGFR therapies. *Mol Cancer Ther* 2016; 15:1106-12.
- Santos C, Azuara D, Garcia-Carbonero R, et al. Optimization of RAS/BRAF mutational analysis confirms improvement in patient selection for clinical benefit to anti-EGFR treatment in metastatic colorectal cancer. *Mol Cancer Ther* 2017; 16:1999-2007.
- Siravegna G, Mussolin B, Buscarino M, et al. Clonal evolution and resistance to EGFR blockade in the blood of colorectal cancer patients. *Nat Med* 2015; 21:795-801.
- Watanabe T, Kobunai T, Yamamoto Y, et al. Heterogeneity of KRAS status may explain the subset of discordant KRAS status between primary and metastatic colorectal cancer. *Dis Colon Rectum* 2011; 54:1170-8.
- Vakiani E, Janakiraman M, Shen R, et al. Comparative genomic analysis of primary versus metastatic colorectal carcinomas. *J Clin Oncol* 2012; 30:2956-62.
- Reiter JG, Makohon-Moore AP, Gerold JM, et al. Minimal functional driver gene heterogeneity among untreated metastases. *Science* 2018; 361:1033-7.
- del Carmen S, Sayagués JM, Bengoechea O, et al. Spatio-temporal tumor heterogeneity in metastatic CRC tumors: a mutational-based approach. *Oncotarget* 2018; 9:34279-88.
- Dienstmann R, Elez E, Argiles G, et al. Analysis of mutant allele fractions in driver genes in colorectal cancer—biological and clinical insights. *Mol Oncol* 2017; 11:1263-72.

43. Tan IB, Malik S, Ramnarayanan K, et al. High-depth sequencing of over 750 genes supports linear progression of primary tumors and metastases in most patients with liver-limited metastatic colorectal cancer. *Genome Biol* 2015; 16:32.
44. Kim KP, Kim JE, Hong YS, et al. Paired primary and metastatic tumor analysis of somatic mutations in synchronous and metachronous colorectal cancer. *Cancer Res Treat* 2017; 49:161-7.
45. Fujiyoshi K, Yamamoto G, Takahashi A, et al. High concordance rate of KRAS/BRAF mutations and MSI-H between primary colorectal cancer and corresponding metastases. *Oncol Rep* 2017; 37:785-92.
46. Joung JG, Oh BY, Hong HK, et al. Tumor heterogeneity predicts metastatic potential in colorectal cancer. *Clin Cancer Res* 2017; 23:7209-16.
47. Brunsell TH, Cengija V, Sveen A, et al. Heterogeneous radiological response to neoadjuvant therapy is associated with poor prognosis after resection of colorectal liver metastases. *Eur J Surg Oncol* 2019; 45:2340-6.
48. Folprecht G, Gruenberger T, Bechstein W, et al. Survival of patients with initially unresectable colorectal liver metastases treated with FOLFOX/cetuximab or FOLFIRI/cetuximab in a multidisciplinary concept (CELIM study). *Ann Oncol* 2014; 25:1018-25.

## Appendix A

### MUTATION DETECTION USING SANGER SEQUENCING

The tissue samples (15-30 mg) were homogenized in liquid nitrogen before DNA extraction. DNA was extracted using the Qiagen AllPrep DNA/RNA/miRNA Universal Kit (catalog no. 80224; Qiagen, Hilden, Germany) standard manual protocol, with the addition of 2 washing steps. The DNA concentration was determined using the NanoDrop 1000 spectrophotometer, version 3.7.1 (Thermo Fisher Scientific, Waltham, MA).

All tumor samples ( $n = 418$ ) were analyzed using Sanger sequencing of *BRAF* exon 15, *KRAS*, and *NRAS* exon 2-4 and *PIK3CA* exons 9 and 20. Singleplex polymerase chain reaction (PCR) reactions were used to amplify *PIK3CA* and *KRAS* exon 2 in a 25- $\mu$ L reaction mix containing 10 $\times$  HotStar-buffer, dNTP (deoxynucleoside triphosphate), and HotStar Taq polymerase, in addition to 50 ng of DNA and primers, as described in Supplemental Table 1 (available in the online version). *NRAS*, *BRAF* exon 15, and *KRAS* exons 3 and 4 were amplified in multiplex PCR reactions with the Qiagen 2 $\times$  Multiplex PCR kit. The PCR products were purified using ExoStar 1-step before Big-Dye Terminator, version 1.1. The Cycle Sequencing Kit and 3730 DNA Analyzer were used for sequencing (Applied Biosystems, Waltham, MA); premix (Big Dye Terminator, version 1.1) buffers (5 $\times$  BDT sequencing buffer) and primers were added. DNA from blood samples from 2 healthy donors was used as controls. The results were analyzed using the Sequencing Analysis software, version 5.3.1, and SeqScape software, version 2.5 (Applied Biosystems). The results were scored independently by 2 observers. All mutations were validated using an independent PCR and forward and reverse sequencing. When discordant results were found between lesions from the same patient (inter-tumor heterogeneity), all results, including the wild-type results, were verified with a second run. If discordance was still present in the mutation profile, the samples were analyzed using next-generation sequencing and droplet digital PCR (ddPCR).

### Mutation Detection by Targeted Sequencing

A total of 47 samples were submitted to ultra-deep targeted sequencing of *KRAS*, *NRAS*, *BRAF*, and *PIK3CA* included in the Illumina TruSight Tumor 15 gene panel (Illumina, San Diego, CA).

Sample preparation was performed in accordance with the protocol. In brief, by amplifying and tagging 25 ng of gDNA for library A and library B per sample, before indexing, purification, and quality controls. All libraries had size distributions in line with the recommendations, with concentrations much greater than 20 ng/ $\mu$ L and a size distribution peak of  $\sim 300$  bp. The libraries were normalized, pooled, denatured, and diluted in accordance with the protocol, except for the pooling of 16 samples, rather than 8 as suggested by the vendor. The 16-sample library pools were sequenced on an Illumina MiniSeq using a high-throughput protocol, with 300 cycles per kit and an average of 89.1% reads per passing filter. Raw fastq files were aligned to the human genome reference (hg19) using the Burrows-Wheeler aligner, version 0.7.5a, in maximum exact matches mode. Sequence alignment map files were sorted and converted to binary alignment map files using the

Picard software package, version 1.102, and variants were called using the SAMtools, version 1.1, mpileup function.

### Mutation Detection Using Exome Sequencing

From the 17 patients with biobanked primary tumor and liver metastasis samples, the data regarding *KRAS*, *NRAS*, *BRAF*, and *PIK3CA* mutations were extracted from the existing exome sequencing data (24 primary tumor samples; 89 liver metastasis samples). Matched normal colonic mucosa was used as a normal control. The exome sequencing data have not been reported but were performed as previously described.<sup>1</sup>

### Mutation Detection Using ddPCR

Mutation detection using ddPCR was performed in 36 samples with BioRad ddPCR Assays (BioRad, Hercules, CA; mutation assays are presented in Supplemental Table 2; available in the online version). A total of 50 ng of DNA from tumor samples was used as the input per well. DNA from the SW48 colon cancer cell line was used as a negative control (wild-type positive). For a positive control, DNA from mutation-positive lesions as detected by Sanger sequencing from the corresponding patients was used (mutation-positive). Finally, water was used as a nontemplate control. The PCR reaction mix and PCR program were set up as recommended by the vendor, including ddPCR Supermix (without UTP) for probes and primer/probe mix labeled with fluorescein (FAM) and hexachlorofluorescein (HEX) fluorophores for target and reference sequences, respectively. The experiments were performed using a QX200 Droplet Digital PCR system (BioRad), consisting of a T100 Thermal cycler for PCR, a QX200 Droplet Generator, and a QX200 Droplet Reader. The results were analyzed and visualized using QuantaSoft, version 1.7.4, software (BioRad). Two replicates per tumor sample were analyzed and merged. Calculation of the absolute number of positive events for a given channel (FAM or HEX) and the fractional abundance of mutation for each sample were performed using the QuantaSoft software. The fractional abundance of the mutant allele was obtained by dividing the number of copies per microliter of mutant allele (FAM channel) by the total copies per microliter of wild-type allele (HEX plus mutant allele (FAM):  $[A/(A + B)]$ ). A total of 50 ng of DNA contains  $\sim 15,000$  haploid genomes, resulting in a detection sensitivity down to a 0.02% allele frequency of mutations in optimal conditions. The software provides mutation scoring using the comparison of the merged results of 2 replicates with fractional abundance of positive droplets in the negative control. The average number of accepted droplets was 20,109 per well.

### Diagnostic Sequencing in Formalin-fixed Tissue

For EGFR antibody treatment guidance for metastatic CRC, a total of 69 primary tumors had been analyzed in the diagnostic laboratory of our pathology department for the detection of *KRAS*, *NRAS*, and *BRAF* mutations, with a detection limit of 1% to 10% of mutant allele frequency. The methods used included allele-specific real-time PCR (*BRAF* V600E/K; *KRAS* codons 12, 13, 61, 117, and 146), pyrosequencing (*NRAS* codons 12, 13, and 61;

*BRAF* codon 464-469 and 600; Therascreen Pyro Kit; Qiagen) and melting curve analysis (*KRAS* codons 12, 13, and 61; Cobas test, Roche Diagnostics).

#### *Microsatellite Instability Testing*

Microsatellite instability (MSI) status was determined in all tumor samples from both primary tumors and liver metastases from the 106 patients ( $n = 418$ ) by analyzing the mononucleotide repeats BAT-25 and BAT-26, as previously described.<sup>2,3</sup> These 2 markers have the capability of identifying 97% of MSI cases.<sup>4</sup> If the results were inconclusive, the samples were analyzed for 5 markers (BAT-25, BAT-26, NR-21, NR-24, MONO-27) with the MSI Analysis System, version 1.2 (Promega), in accordance with the manufacturer's instructions.

#### *Excluded Samples*

In 7 tumor samples from 5 patients with mutations detected in other samples, no mutations were detected using Sanger sequencing or the targeted next-generation sequencing panel analyzing 15 cancer-related genes. These samples were also analyzed using ddPCR without detecting the same mutations detected in the corresponding liver metastases. High-resolution allele-specific DNA copy number data (Affymetrix CytoScan HD SNP Array) was available for all but 1 sample and showed a diploid profile clearly different from that of the other metastases from the same patients. Thus, it is likely that the sample had been taken from an area without viable tumor tissue and that the absence of mutations reflected a low tumor cell count; hence, these samples were excluded.

# RAS/BRAF/PIK3CA Mutations in Multiple CRLMs

**Supplemental Table 1** Primers Used for Sanger Sequencing

Gene	Exons	Product Size	Forward Primer (5'-3')	Reverse Primer (5'-3')	Annealing Temperature	Cycles, n
<i>BRAF</i>	15	224	tcataatgctgctctgatagga	ggccaaaaatataatcagtgga	59°C	35
<i>KRAS</i>	2	256	actggtggagatttgatag	gtatcaagaatggtcct	50°C	35
	3	244	ccagactgtgttctcccttc	actcctaatgctcagcttattatc	59°C	35
	4	390	tgacaaaagttgtggacaggt	aagaagcaatgccctctcaa	59°C	35
<i>NRAS</i>	2	227	tactgtagatgggctcgcc	ccgacaagtgagagacagga	59°C	35
	3	300	attgaactccctccctccc	tgtgtaacctcattcccca	59°C	35
	4	238	gcctaactgttttcttatgtctg	cttgacaaatgctgaaagc	59°C	35
<i>PIK3CA</i>	9	487	gattggtcttccctgctctg	ccacaaatcaatttacaccattg	58°C	35
	20	805	aagcctctctaattttgtgac	aaactccagtttactacacc	54°C	35

**Supplemental Table 2** Mutation Assays Used for Droplet Digital PCR

Mutation Assay	Assay ID	Fluorophore
KRAS p.G12D	dHsaCP2000001	FAM
KRAS WT for p.G12D	dHsaCP2000002	HEX
KRAS p.G13C	dHsaCP2500594	FAM
KRAS WT for p.G13C	dHsaCP2500595	HEX
KRAS p.A146T	dHsaCP2000079	FAM
KRAS WT for p.A146T	dHsaCP2000080	HEX
NRAS p.G12D	dHsaCP2000095	FAM
NRAS WT for p.G12D	dHsaCP2000096	HEX
PIK3CA p.E545K	dHsaCP2000075	FAM
PIK3CA WT for p.E545K	dHsaCP2000076	HEX
BRAF p.V600E	dHsaCP2000027	FAM
BRAF WT for p.V600E	dHsaCP2000028	HEX

Abbreviations: FAM = fluorescein; HEX = hexachlorofluorescein; ID = identification; PCR = polymerase chain reaction; WT = wild-type.

**Supplemental Table 3** Data From All Patients With Number of Biobanked Samples and Mutation Status According to Sanger Sequencing and Diagnostic Sequencing<sup>a</sup>

Pt. No.	Sanger Sequencing					Diagnostic Sequencing		
	Biobanked Metastasis Samples, n	Total Samples, n	<i>KRAS</i> , <i>NRAS</i> , <i>BRAF</i> , <i>PIK3CA</i> Mutation	Mutation Type	Mutation Fraction <sup>b</sup>	<i>KRAS</i> Diagnostic	<i>NRAS</i> Diagnostic	<i>BRAF</i> Diagnostic
1	2 + PT	3	<i>KRAS</i>	G12D	0.67	Mutation (liver)		WT
			<i>PIK3CA</i>	E545K	0.33			
2	4	4	<i>KRAS</i>	G12D	0.75	Mutation	WT	WT
			<i>PIK3CA</i>	E545K	0.75			
3	7	7	<i>KRAS</i>	G12D	1			
			<i>PIK3CA</i>	E545K	0.14			
4	2	2	<i>KRAS</i>	G12D	1	Mutation		
			<i>PIK3CA</i>	E545K	1			
5	5	5	<i>KRAS</i>	G12D	1	Mutation		WT
			<i>PIK3CA</i>	Q546E	1			
6	3	3	<i>KRAS</i>	G12D	1	Mutation		
			<i>PIK3CA</i>	H1047R	1			
7	5	5	<i>KRAS</i>	G12S	0.80	Mutation		
			<i>PIK3CA</i>	H1047R	0.60			
8	1 + PT	2	<i>KRAS</i>	G12V	1	Mutation (lung)		
			<i>PIK3CA</i>	E545K	1			
9	2	2	<i>KRAS</i>	G12V	1			
			<i>PIK3CA</i>	E545K	1			
10	3	3	<i>KRAS</i>	G12V	1			
			<i>PIK3CA</i>	E545K	1			
11	5	5	<i>KRAS</i>	G12V	1	Mutation		
			<i>PIK3CA</i>	E545K	0.80			
12	3	3	<i>KRAS</i>	G12C	1			
			<i>PIK3CA</i>	E545K	1			
13	2	2	<i>KRAS</i>	G12C	1			
			<i>PIK3CA</i>	Q546R	0.50			
14	2	2	<i>KRAS</i>	G13D	1	Mutation	WT	WT
			<i>PIK3CA</i>	E542K	1			
15	5	5	<i>KRAS</i>	G13D	1	Mutation		
			<i>PIK3CA</i>	E545A	0.40			
16	4	4	<i>KRAS</i>	G12D	0.25	Mutation	WT	WT
17	3	3	<i>KRAS</i>	G12D	1	Mutation		
18	4	4	<i>KRAS</i>	G12D	1			

Supplemental Table 3 Continued

Pt. No.	Sanger Sequencing					Diagnostic Sequencing		
	Biobanked Metastasis Samples, n	Total Samples, n	<i>KRAS</i> , <i>NRAS</i> , <i>BRAF</i> , <i>PIK3CA</i> Mutation	Mutation Type	Mutation Fraction <sup>b</sup>	<i>KRAS</i> Diagnostic	<i>NRAS</i> Diagnostic	<i>BRAF</i> Diagnostic
19	6	6	<i>KRAS</i>	G12D	1	Mutation		
20	9	9	<i>KRAS</i>	G12D	1	Mutation (liver)	WT	WT
21	1 + PT	5	<i>KRAS</i>	G12D	1	Mutation	WT	WT
22	2	2	<i>KRAS</i>	G12D	1			
23	2	2	<i>KRAS</i>	G12D	1	Mutation		WT
24	1 + PT	5	<i>KRAS</i>	G12D	1	Mutation		
25	4	4	<i>KRAS</i>	G12V	1	Mutation		WT
26	2	2	<i>KRAS</i>	G12V	1			
27	7 + PT	10	<i>KRAS</i>	G12V	1	Mutation		
28	3	3	<i>KRAS</i>	G12V	1	Mutation		
29	4 + Rec	5	<i>KRAS</i>	G12V	1	Mutation	WT	WT
30	3	3	<i>KRAS</i>	G12V	1	Mutation		
31	2	2	<i>KRAS</i>	G12V	1	Mutation		
32	5	5	<i>KRAS</i>	G12V	1	Mutation		WT
33	4	4	<i>KRAS</i>	G12C	1	Mutation		
34	2	2	<i>KRAS</i>	G12C	1	Mutation		
35	2	2	<i>KRAS</i>	G12C	1	Mutation		
36	8	8	<i>KRAS</i>	G12C	1	Mutation		
37	4	4	<i>KRAS</i>	G12C	1	Mutation	WT	WT
38	5 + PT	9	<i>KRAS</i>	G12A	1	Mutation		
39	3	3	<i>KRAS</i>	G12A	1			
40	1 + PT	6	<i>KRAS</i>	G12A	1			
41	2	2	<i>KRAS</i>	G12S	1	WT <sup>c</sup>		
42	1 + PT	2	<i>KRAS</i>	G12S	1	Mutation		
43	5	5	<i>KRAS</i>	G13C	0.60	Mutation	WT	WT
44	3	3	<i>KRAS</i>	G13C	0.67	WT (liver) <sup>d</sup>	WT	WT
45	5	5	<i>KRAS</i>	G13D	0.80	Mutation		
46	6	6	<i>KRAS</i>	G13D	1			
47	1 + PT	3	<i>KRAS</i>	A146T	0.67			
48	3	3	<i>KRAS</i>	Q61H	1			
49	3	3	<i>KRAS</i>	Q61R	1			
50	2	2	<i>KRAS</i>	Q61R	0.50	Mutation		
51	2	2	<i>KRAS</i>	K117N	1	WT <sup>c</sup>	WT	WT
52	4	4	<i>KRAS</i>	A146T	1	WT <sup>c</sup>	WT	WT

**Supplemental Table 3** Continued

Pt. No.	Sanger Sequencing					Diagnostic Sequencing		
	Biobanked Metastasis Samples, n	Total Samples, n	<i>KRAS</i> , <i>NRAS</i> , <i>BRAF</i> , <i>PIK3CA</i> Mutation	Mutation Type	Mutation Fraction <sup>b</sup>	<i>KRAS</i> Diagnostic	<i>NRAS</i> Diagnostic	<i>BRAF</i> Diagnostic
53	1 + PT + Rec	3	( <i>KRAS</i> )	(D33E)	1	WT	WT	WT
54	1 + PT	6	<i>NRAS</i>	G12D	1			
55	4	4	<i>NRAS</i>	G12D	0.50	WT	Mutation	WT
56	3 + PT	6	<i>NRAS</i>	G12V	0.67	WT	Mutation	WT
57	5	5	<i>NRAS</i>	Q61K	1			
58	5	5	<i>NRAS</i>	Q61K	1			
59	4	4	<i>NRAS</i>	Q61R	1			
60	2 + PT	3	<i>BRAF</i>	D594G	1	WT (liver) <sup>d</sup>	WT	WT
61	3	3	<i>BRAF</i>	D594G	1	WT	WT	WT
62	3	3	<i>BRAF</i>	V600E	1			
63	2	2		WT <sup>c</sup>		Mutation		
64	2	2		WT <sup>c</sup>		WT	Mutation	WT
65	4	4		WT <sup>c</sup>		WT	WT	Mutation
66	2	2		WT		WT	WT	WT
67	2	2		WT		WT	WT	WT
68	2	2		WT		WT	WT	WT
69	2	2		WT		WT	WT	WT
70	2	2		WT		WT	WT	WT
71	2	2		WT		WT	WT	WT
72	3	3		WT		WT	WT	WT
73	3	3		WT		WT	WT	WT
74	3	3		WT		WT	WT	WT
75	4	4		WT		WT	WT	WT
76	4	4		WT		WT	WT	WT
77	4	4		WT		WT	WT	WT
78	4	4		WT		WT	WT	WT
79	4	4		WT		WT	WT	WT
80	5	5		WT		WT	WT	WT
81	5	5		WT		WT	WT	WT
82	5	5		WT		WT	WT	WT
83	5	5		WT		WT	WT	WT
84	5	5		WT		WT	WT	WT
85	5	5		WT		WT	WT	WT
86	5	5		WT		WT (liver)	WT	WT



Supplemental Table 3 Continued								
Pt. No.	Sanger Sequencing					Diagnostic Sequencing		
	Biobanked Metastasis Samples, n	Total Samples, n	<i>KRAS</i> , <i>NRAS</i> , <i>BRAF</i> , <i>PIK3CA</i> Mutation	Mutation Type	Mutation Fraction <sup>b</sup>	<i>KRAS</i> Diagnostic	<i>NRAS</i> Diagnostic	<i>BRAF</i> Diagnostic
87	5	5		WT		WT	WT	WT
88	5	5		WT		WT	WT	WT
89	5 + PT + Rec	7		WT		WT (liver)	WT	WT
90	5 + PT + Rec	12		WT		WT	WT	WT
91	3	3		WT		WT	WT	WT
92	2	2		WT		WT		WT
93	5	5		WT		WT		WT
94	5 + Rec	6		WT		WT		WT
95	6	6		WT		WT		WT
96	1 + PT	2		WT				
97	2 + PT	5		WT				
98	3 + Rec	4		WT				
99	2 + Rec	3		WT				
100	2	2		WT				
101	2	2		WT				
102	2	2		WT				
103	3	3		WT				
104	4	4		WT				
105	4	4		WT				
106	5	5		WT				

Empty cells mean that patient tumor samples have not been tested in the diagnostic setting.

Abbreviations: PT = primary tumor; Pt. No. = patient number; Rec = recurrence of liver metastases; WT = wild-type.

<sup>a</sup>For 7 patients, diagnostic formalin-fixed paraffin-embedded testing was performed using metastatic tissue (6 liver samples and 1 lung sample).

<sup>b</sup>Mutation fraction reflects the inpatient mutation frequency of tumor samples using Sanger sequencing.

<sup>c</sup>Discordance between diagnostic testing and Sanger sequencing.

<sup>d</sup>Analyzed using a mutation assay that did not include this specific mutation.

**Supplemental Table 4** Overview of Results of Sensitive Mutation Detection (Targeted/Exome Next-generation Sequencing) for All Patients With Heterogeneous Mutations Detected Using Sanger Sequencing

Variable			Sanger Score	NGS					ddPCR					Final Score	
				%	T	C	G	A	%	Score	Alt	Ref	Alt		Ref
Intra-patient heterogeneity			Exome sequencing												
Pt 47	KRAS Ala146Thr	Primary	WT <sup>a</sup>	0	0 <sup>b</sup>	74	0	0	0.02	WT	3	10,309	3	6437	WT <sup>a</sup>
		T1-1	Mut	23	12 <sup>b</sup>	40	0	0	30	Mut	2098	5201			Mut
		T1-2	Mut	31	15 <sup>b</sup>	33	0	0	40	Mut	3500	6251			Mut
Pt 1	PIK3CA Glu545Lys	Primary	WT <sup>a</sup>	0	0	0	107	0 <sup>b</sup>	0.06	WT	6	10,568	12	8325	WT <sup>a</sup>
		T1	Mut	13	0	0	53	8 <sup>b</sup>	30	Mut	3676	5371			Mut
		T2	WT <sup>a</sup>	6.1	0	0	107	7 <sup>b</sup>	4.8	Mut	505	7304			Mut <sup>c</sup>
	KRAS Gly12Asp	Primary	Mut	44	57 <sup>b</sup>	73	0	0							Mut
		T1	Mut	49	50 <sup>b</sup>	53	0	0							Mut
		T2	WT <sup>a</sup>	4.1	7 <sup>b</sup>	162	0	0							Mut <sup>c</sup>
Pt 56	NRAS Gly12Val	Primary	Mut	19	0	80	0	19 <sup>b</sup>							Mut
		T1-1	WT <sup>a</sup>	4.8	0	79	0	4 <sup>b</sup>							Mut <sup>c</sup>
		T1-2	WT <sup>a</sup>	4.2	0	91	0	4 <sup>b</sup>							Mut <sup>c</sup>
		T2	Mut	34	0	42	0	22 <sup>b</sup>							Mut
		T4-1	Mut	8.1	0	124	0	11 <sup>b</sup>							Mut
		T4-2	Mut	7.3	0	102	0	8 <sup>b</sup>							Mut
Primary-to-metastatic heterogeneity <sup>d</sup>			Targeted sequencing												
Pt 65	BRAF V600E	T1	WT <sup>a</sup>	0.26	97 <sup>b</sup>	11	15	37,805	0.08	Mut	13	8422	4	7265	Mut <sup>c</sup>
		T2	WT <sup>a</sup>	1.2	467 <sup>b</sup>	13	23	37,244	0.9	Mut	84	6807	88	7309	Mut <sup>c</sup>
		T3	WT <sup>a</sup>	0.20	67 <sup>b</sup>	6	13	32,858	0.3	Mut	30	5150	52	12,285	Mut <sup>c</sup>
		T4-1	WT <sup>a</sup>	0.10	29 <sup>b</sup>	8	28	29,900	0.01	Mut	1	11,621	4	9256	WT <sup>a</sup>

Supplemental Table 4 Continued															
Primary-to-metastatic heterogeneity <sup>d</sup>				Targeted sequencing											
Pt 63	KRAS Gly12Asp	T2-1	WT <sup>a</sup>	0.60	50 <sup>b</sup>	8278	4	13	1.4	Mut	75	5238	109	5503	Mut <sup>c</sup>
		T4	WT <sup>a</sup>	0.15	11 <sup>b</sup>	7392	12	18	0.07	WT	6	6523	6	6033	WT <sup>f</sup>
Pt 64	NRAS Gly12Cys	T1-1	WT <sup>a</sup>	0.37	2	16,315	19	60 <sup>b</sup>							Mut <sup>c</sup>
		T2	WT <sup>a</sup>	1.4	5	17,884	22	259 <sup>b</sup>							Mut <sup>c</sup>
Inter-metastatic heterogeneity				Targeted sequencing											
Pt 2	KRAS Gly12Asp	T1-1	Mut	42	4709 <sup>b</sup>	6536	9	18	42	Mut	5646	7531			Mut
		T2	Mut						21	Mut	1019	4156			Mut
		T3	Mut						28	Mut	1944	5438			Mut
		T4	WT <sup>a</sup>	0.16	16 <sup>b</sup>	10,051	12	15	0.13	Mut	17	9433	32	13,073	WT <sup>e</sup>
	PIK3CA Glu545Lys	T1-1	Mut	47	35	10	7855	6943 <sup>b</sup>	44	Mut	6188	7715			Mut
		T2	Mut						22	Mut	1349	4887			Mut
		T3	Mut						29	Mut	1750	4453			Mut
		T4	WT <sup>a</sup>	0.04	38	30	14,460	6 <sup>b</sup>	0.12	WT	11	6468	12	7619	WT <sup>e</sup>
Pt 7	KRAS Gly12Ser	T1	Mut	16	967 <sup>b</sup>	5137	4	14							Mut
		T2	WT <sup>a</sup>	0.66	56 <sup>b</sup>	7916	17	20							Mut <sup>c</sup>
		T3-1	Mut	36	3498 <sup>b</sup>	6895	4	16							Mut
		T4	Mut												Mut
		T5	Mut												Mut
	PIK3CA His1047Arg	T1	WT <sup>a</sup>	9.6	30	8	3180 <sup>b</sup>	29,259							Mut <sup>c</sup>
		T2	WT <sup>a</sup>	0.43	31	12	277 <sup>b</sup>	45,262							Mut <sup>c</sup>
		T3-1	Mut	19	50	32	11,067 <sup>b</sup>	42,509							Mut
		T4	Mut												Mut
		T5	Mut												Mut
Pt 13	KRAS Gly12Cys	T1-1	Mut	42	2	2194	0	1604 <sup>b</sup>							Mut
		T2-1	Mut	19	1	3610	0	829 <sup>b</sup>							Mut
	PIK3CA Gln546Arg	T1-1	Mut	36	3	1	1704 <sup>b</sup>	3073							Mut
T2-1		WT <sup>a</sup>	5.4	1	1	318 <sup>b</sup>	5545							Mut <sup>c</sup>	

**Supplemental Table 4** Continued

Inter-metastatic heterogeneity				Targeted sequencing												
Pt 50	KRAS Glu61Arg	T1-1	WT <sup>a</sup>	18	6531	1467	2	17								Mut <sup>c</sup>
		T2	Mut	29	5660	2351	3	6								Mut
Pt 44	KRAS Gly13Cys	T1-1	Mut	15	0	3658	0	649								Mut
		T2-1	Mut	9.4	0	3148	0	326								Mut
		T3	WT <sup>a</sup>	8.9	1	3938	2	384								Mut <sup>c</sup>
Pt 3	KRAS Gly12Asp	T1-1	Mut	75	5953 <sup>b</sup>	2035	5	11								Mut
		T2	Mut	72	5767 <sup>b</sup>	2240	4	2								Mut
		T3-1	Mut	65	4945 <sup>b</sup>	2706	7	8								Mut
		T4-1	Mut	56	2389 <sup>b</sup>	1887	1	0								Mut
		T5-1	Mut	75	6012 <sup>b</sup>	1989	3	5								Mut
		T7-1	Mut	65	5229 <sup>b</sup>	2769	2	5								Mut
		T9-1	Mut	73	5855 <sup>b</sup>	2151	4	2								Mut
	PIK3CA Glu545Lys	T1-1	WT <sup>a</sup>	0.03	19	19	11,123	3 <sup>b</sup>	0.02	WT	2	6683	2	6491	WT <sup>a</sup>	
		T2	WT <sup>a</sup>	0	36	36	17,487	0 <sup>b</sup>	0.01	WT	0	5736	2	6713	WT <sup>a</sup>	
		T3-1	WT <sup>a</sup>	0.03	27	29	11,910	3 <sup>b</sup>	0.05	WT	3	6237	5	6760	WT <sup>a</sup>	
		T4-1	Mut	45	19	17	4196	3477 <sup>b</sup>	24	Mut	2753	7424	2565	6955	Mut	
		T5-1	WT <sup>a</sup>	0.01	43	25	15,715	2 <sup>b</sup>	0.02	WT	2	6454	1	7126	WT <sup>a</sup>	
		T7-1	WT <sup>a</sup>	0.04	27	10	13,072	5 <sup>b</sup>	0.01	WT	2	6600	0	6395	WT <sup>a</sup>	
		T9-1	WT <sup>a</sup>	0	22	28	14,501	0 <sup>b</sup>	0.02	WT	1	4537	1	5211	WT <sup>a</sup>	
Pt 15	KRAS Gly13Asp	T1-1	Mut	18	889 <sup>b</sup>	3986	1	6								Mut
		T2-1	Mut													Mut
		T3-1	Mut	39	2141 <sup>b</sup>	3348	1	6								Mut
		T4	Mut	16	820 <sup>b</sup>	4375	1	5								Mut
		T5	Mut	17	878 <sup>b</sup>	4324	1	11								Mut
	PIK3CA Glu545Ala	T1-1	WT <sup>a</sup>	0.09	27	14 <sup>b</sup>	2	15,134								WT <sup>a</sup>
		T2-1	Mut													Mut
		T3-1	Mut	50	25	6761 <sup>b</sup>	7	6782							Mut	
		T4	WT <sup>a</sup>	0.11	16	17 <sup>b</sup>	4	15,993							WT <sup>a</sup>	
		T5	WT <sup>a</sup>	0.08	21	13 <sup>b</sup>	6	16,225							WT <sup>a</sup>	

Supplemental Table 4 Continued

Inter-metastatic heterogeneity				Targeted sequencing												
Pt 11	KRAS Gly12Val	T1-1	Mut	19	4	3586	0	815 <sup>b</sup>								Mut
		T3-1	Mut	47	5	3260	4	2837 <sup>b</sup>								Mut
		T4-1	Mut													Mut
		T5-1	Mut													Mut
		T6	Mut													Mut
	PIK3CA Glu545Lys	T1-1	WT <sup>a</sup>	16	3	8	5351	982 <sup>b</sup>								Mut <sup>c</sup>
		T3-1	Mut	61	0	3	2937	4516 <sup>b</sup>								Mut
		T4-1	Mut													Mut
		T5-1	Mut													Mut
		T6	Mut													Mut
Pt 55	NRAS Gly12Asp	T1-1	Mut	87	17,113 <sup>b</sup>	2636	17	16	86	Mut	4959	5273				Mut
		T2	Mut						17	Mut	1304	5701				Mut
		T3	WT <sup>a</sup>	0.04	10 <sup>b</sup>	22,693	45	42	0.04	WT	3	6714	4	6426		WT <sup>e</sup>
		T4	WT <sup>a</sup>	0.08	11 <sup>b</sup>	14,422	31	24	0.03	WT	5	9422	4	9230		WT <sup>e</sup>
Pt 43	KRAS Gly13Cys	T1	WT <sup>a</sup>	0.3	4	7834	7	25 <sup>b</sup>	0	WT	0	7050	0	7667		WT <sup>e</sup>
		T2	WT <sup>a</sup>	0.2	2	7417	8	15 <sup>b</sup>	0	WT	0	7673	0	6987		WT <sup>e</sup>
		T3	Mut	74	1	2110	6	6026 <sup>b</sup>	72	Mut	4224	5114				Mut
		T4	Mut						41	Mut	2712	5148				Mut
		T5	Mut						27	Mut	1903	5394				Mut
Pt 16	KRAS Gly12Asp	T1-1	Mut	8.4	614 <sup>b</sup>	6684	6	16	6.7	Mut	292	3698				Mut
		T2-1	WT <sup>a</sup>	2.7	192 <sup>b</sup>	6825	12	10	2.6	Mut	236	6362	201	6340		Mut <sup>c</sup>
		T3	WT <sup>a</sup>	4.4	275 <sup>b</sup>	5957	8	11	3.9	Mut	1007	12,170	981	12,617		Mut <sup>c</sup>
		T4	WT <sup>a</sup>	0.7	45 <sup>b</sup>	6303	11	15	0.5	Mut	39	5961	49	6774		Mut <sup>c</sup>
Pt 45	KRAS Gly13Asp	T1-1	WT <sup>a</sup>	4.8	218 <sup>b</sup>	4365	0	3								Mut <sup>c</sup>
		T2-1	Mut	69	3718 <sup>b</sup>	1638	1	3								Mut
		T4-1	Mut													Mut
		T6-1	Mut													Mut
		T7	Mut												Mut	

Abbreviations: A = adenine; Alt = alternative; C = cytosine; ddPCR = droplet digital polymerase chain reaction; G = guanine; NGS = next-generation sequencing; Mut = mutation; Pt = patient; Ref = reference; T = thymine; WT = wild-type.

<sup>a</sup>Discordance in mutation status compared with other tumor samples from the same patient.

<sup>b</sup>Read count of mutated base; read count of normal base and noise also shown.

<sup>c</sup>Concordance in mutation status compared with other tumor samples from the same patient.

<sup>d</sup>Mutations detected in the primary tumor by mutation testing in the diagnostic setting; primary tumor samples microscopically evaluated to contain > 40% tumor cells.

<sup>e</sup>No copy number aberrations, excluded because of assumed low tumor cell count.

<sup>f</sup>Excluded because of assumed low tumor cell count.

## Supplemental References

1. Sveen A, Johannessen B, Tengs T, et al. Multilevel genomics of colorectal cancers with microsatellite instability—clinical impact of JAK1 mutations and consensus molecular subtype 1. *Genome Med* 2017; 9:46.
2. De Sousa E Melo F, Wang X, Jansen M, et al. Poor-prognosis colon cancer is defined by a molecularly distinct subtype and develops from serrated precursor lesions. *Nat Med* 2013; 19:614-8.
3. Merok MA, Ahlquist T, Røyrvik EC, et al. Microsatellite instability has a positive prognostic impact on stage II colorectal cancer after complete resection: results from a large, consecutive Norwegian series. *Ann Oncol* 2013; 24:1274-82.
4. Cicek MS, Lindor NM, Gallinger S, et al. Quality assessment and correlation of microsatellite instability and immunohistochemical markers among population- and clinic-based colorectal tumors results from the Colon Cancer Family Registry. *J Mol Diagn* 2011; 13:271-81.